Appl. Phys. B (2015) 118:85–92
DOI 10.1007/s00340-014-5957-0

Applied Physics B
Lasers and Optics

On the quantitative absorption and Stokes shift in PbSe quantum dots embedded in glasses

De-Wei Ma · Hui-Lv Jiang · Cheng Cheng

Received: 26 March 2014 / Accepted: 30 October 2014 / Published online: 8 November 2014

Abstract The synthesis of PbSe quantum dots (QDs) in silicate glasses was achieved by a simple melt-annealing technique. Transmission electron microscopy analysis proves the formation of PbSe QDs in glasses. The absorption spectra show that the light absorption originates from the PbSe QDs in glasses mostly, and the energy-integrated molar extinction coefficient for the first exciton transition was deemed to be only about 1/10 of those from colloidal PbSe QDs. The photoluminescence analysis reveals that the Forster energy transfer is responsible for the shape of the PL peak. For the sample with PbSe QDs in a small radius of 5.2 nm, a pronounced Stokes shift of 70 meV was found, and the Huang–Rhys factor was calculated to be 2.1.

1 Introduction

Semiconductors in nano-crystallized form exhibit markedly different electrical, optical and structural properties as compared to those in the bulk form [1, 2]. Quantum dots (QDs), confined in all three spatial dimensions, are fascinating systems demonstrating three-dimensional quantum confinement effects as the nanocrystal sizes approach the exciton Bohr radii. Particularly, their optical properties differ greatly from those of the corresponding molecular and bulk materials, and the quantum confinement effect makes QDs exhibiting tunable optical absorption and emission properties with varying dot size, reflecting not only in the peak wavelengths, but also in the absorption and emission coefficients.

IV–VI semiconductor PbSe possesses a narrow bandgap of 0.278 eV and an exciton Bohr radius of 46 nm, much larger than those of II–VI cadmium chalocogenide (4–10 nm). And the optical spectra of PbSe QDs can cover a wide near-infrared (NIR) waveband range of 1–3 μm by altering the QD size, which is very important for optical communication applications. The very large Bohr radius permits the optical properties of PbSe QDs to be evaluated in the limit of extremely strong quantum confinement because the strong confinement effect can be obtained easily with large particles. Meanwhile, the quantum confinement effect would suffer less possible interference from QD surface defects for the large particles, which benefits the enhancement of QDs emission efficiency [3–5].

Various methods have been used to prepare PbSe QDs [4–9]. Current syntheses, such as the one with the organic solution method, can produce high-quality PbSe QDs with respect to photoluminscent (PL) quantum yield in excess of 60 % and size distribution of ±5 % [10, 11]. But for practical applications, QDs should be integrated into surrounding matrices such as polymers or glasses; especially, considering that glass matrices are chemically and mechanically stable and can provide robust materials for fabrication of optoelectronic devices in bulk, planar or fiber forms, and PbSe QDs fused into glass hosts have received much attention in the past two decades [12].

With regard to the applications of PbSe QDs in glasses in optoelectronics, optical studies are undoubtedly important. Previous studies on PbSe [13–17], PbS [18–20], InAs [21] and CdSe [22] QDs mainly concentrated on the colloidal QDs. The absorption coefficient (absorption cross section) defines the extent to which a material absorbs energy. Leatherdale et al. [22] reported that the absorption

D.-W. Ma (✉) · H.-L. Jiang · C. Cheng
Institute of Intelligent Optoelectronic Technology, Zhejiang University of Technology, Hangzhou 310023, People's Republic of China
e-mail: dwma@zjut.edu.cn

cross section of CdSe QDs was largely insensitive to the surrounding solvent. The oscillator strength, depending on intrinsic QD properties merely, was used as a measure to decide the relative strength of the electronic transitions in QDs, and the oscillator strength was found in the range 8–25 depending on QD size for the first exciton transition of the colloidal PbSe QDs [13]. The Maxwell–Garnett (MG) effective medium theory was used to evaluate the absorption coefficient of QDs, and it was found that the calculation results agreed well with the experimental data at high photon energies [13, 20–22]. PL spectra depend on the material properties, and their intensity dependencies can allow one to investigate recombination mechanisms. The shift of the PL band with respect to the absorption-edge is called the Stokes shift. Different groups gave different results for the Stokes shift of PbSe QDs in similar sizes, and the results look inconsistent. For instance, Wehrenberg et al. [16] reported a Stokes shift of 38 nm for the PbSe QDs with a mean size of 4.6 nm; Pietryga et al. [23] reported a Stokes shift of 52 nm for the PbSe QDs with a mean size of 12 nm; and Lifshitz et al. [24] reported a Stokes shift of 133 nm for the PbSe QDs in size of 4 nm and an anti-Stokes photoluminescence (ASPL) of −10 nm for the QDs in a size of 6.3 nm.

Contrary to the quantitative absorption and PL studies on colloidal QDs, there have been few quantitative spectroscopic studies on QDs embedded in glasses; previous studies were mainly devoted to the qualitative descriptions of the absorption and PL results, or related to decay kinetics studies, nonlinear optical behavior, etc. [6, 25–33]. In this paper, we reported synthesis of PbSe QDs in silicate glasses by a melt-annealing technique and emphasized on quantitative studies on the absorption and PL studies of PbSe QDs in silicate glasses. We found that with the increase of thermal-treatment temperature, the generated smaller PbSe QDs would coalesce into bigger ones, which leads to the decrease of QD density in host glass. The absorption spectra show that the light absorption originates from the generated PbSe QDs in glasses mostly, and the calculated energy-integrated absorption coefficient for the first exciton transition is only about 1/10 of those from colloidal PbSe QDs previously reported. And we calculated the oscillator strength per particle of the first optical transition, which is far smaller than 8–25 in previous report [13] possibly due to the existence of substantial surface defects. By the PL studies, we thought that the Forster energy transfer was responsible for the shape of the PL peak. And then, the Stokes shift of the PL peak with respect to the absorption-edge was studied. For the sample with PbSe QDs with a small radius of 5.2 nm, a pronounced shift of 70 meV was found, and the Huang–Rhys factor was calculated to be 2.1.

2 Experimental procedure

The glass compositions were chosen including (in wt%): 58.7 SiO_2, 8.9 ZnO, 15.7 Na_2O, 4.5 B_2O_3, 4.0 Al_2O_3, 2.2 AlF_3, 3.0 PbO, 3.0 Se and an additional 1.0 element C. These materials were mixed together thoroughly and melted for 1 h in a corundum crucible at 1,400 °C in an electrically heated furnace. The glass melts were then quenched by pouring onto metal molds, and glass samples with transparent straw-yellow colors were obtained. According to our previous reports [34], the adequate temperature for the crystallization of PbSe QDs in silicate glass was in the range of 550–650 °C. Therefore, in the following thermal-treatment stage, the glass samples were annealed at 550, 600 and 650 °C, respectively, for 5 h, which were labeled as samples *G*1, *G*2 and *G*3, respectively. As a result, the glasses turned black, indicating the formation of PbSe crystalline phase in the host glasses.

The glass samples were characterized with the help of different characterization techniques. The transmission electron microscope (TEM, Tecnai G2 F30 S-Twin) images were used to study the crystalline quality and morphology of PbSe QDs. The absorption spectra were observed with a Shimadzu UV-3150 UV–VIS–NIR spectrophotometer; the PL spectra were measured with an Edinburgh FLSP920 fluorescence spectrometer, where an Nd^{3+}: YAG laser source with the excitation wavelength of 1,064 nm and the power of 1 W was used.

3 Results and discussion

Firstly, TEM measurements were carried out to study the microstructures and morphologies of the PbSe crystalline phase in host glasses, as illustrated in Fig. 1. It is clearly seen that some nearly spherical black dots are dispersed in the glass matrices in samples *G*1–*G*3. Then, high-resolution TEM (HR-TEM) measurements were used to discriminate the black dots; the insets in Fig. 1 (*G*1–*G*3) show the HR-TEM images of a typical black dot corresponding to each sample. The lattice distances annotated in the HR-TEM images are measured to be 2.16 Å, equal to the distance of neighboring (220) crystal plane of PbSe crystal, which thus proves the precipitation of PbSe QDs in all samples. The EDX spectrum from a typical PbSe QD in the samples further confirms the existence of elements Pb and Se, and no other elements exist inside the QD except for the elements Cu and Zn from TEM grid.

Another phenomenon that should be noted is that in sample *G*1 and *G*2, one black dot usually stands for a single PbSe QD; while in sample *G*3, one seemingly black dot is normally made up of several PbSe QDs, as illustrated in the inset of Fig. 1(*G*3), and at least three kinds of crystal planes

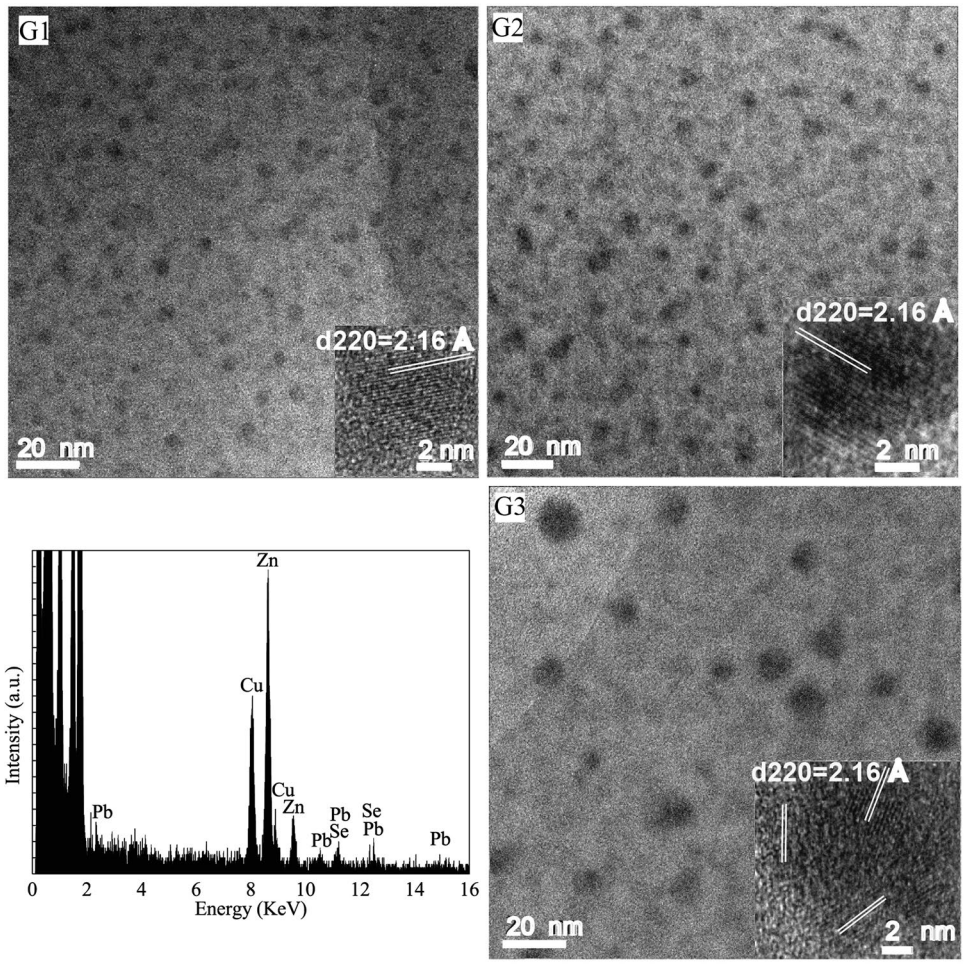

Fig. 1 TEM images of PbSe QDs in sample *G*1, *G*2 and *G*3; the insets are the HR-TEM images of a typical single PbSe QD corresponding to each sample; the EDX spectrum is from a typical PbSe QD in the samples

with different orientations are annotated in this HR-TEM image. This means that this PbSe QD consists of at least three smaller PbSe QDs. Furthermore, we can see from the figures that the QD density in sample *G*3 is evidently smaller than those in sample *G*1 and *G*2. Therefore, we can conclude that with the increase of thermal-treatment temperature, not only do the diffusion velocities of Pb^{2+} and Se^{2-} speed up, promoting the growth of PbSe QDs, but also the generated smaller PbSe QDs would coalesce into bigger ones, hence leading to the decrease of QD density in host glass [35]. For each sample, several TEM images were taken from different areas, and then, the PbSe QDs were counted and measured to give a mean size, which are 4.7, 6.8 and 10.8 nm, respectively, for samples *G*1, *G*2 and *G*3.

Figure 2 shows the linear absorptions of samples *G*1–*G*3. For the sake of comparison, the absorbance curves of the glass sample without PbSe ingredient and the as-prepared PbSe-doped glass sample without thermal-treatment are presented. Evidently, the samples *G*1 and *G*2 have one

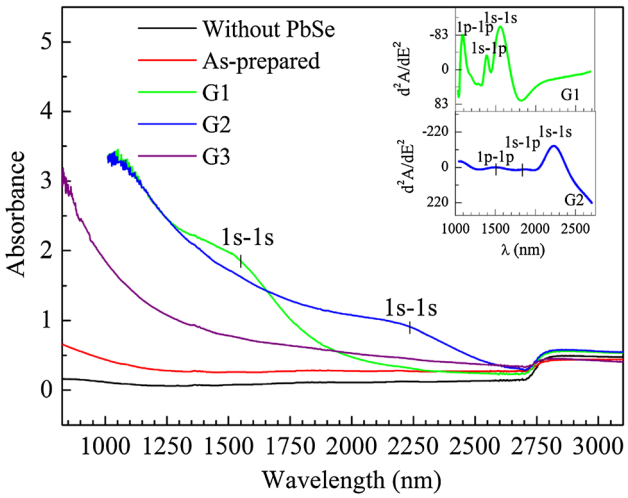

Fig. 2 Optical absorption spectra of glass samples without and with PbSe introductions annealed at different temperatures; the *insets* are the second derivatives of the absorption spectra from samples *G*1 and *G*2

distinct absorption peak near the wavelengths of 1,550 and 2,250 nm, respectively, which are attributed to the first exciton ($1S_h$–$1S_e$) transitions in PbSe QDs for samples *G*1 and *G*2. Generally, the QD size will get larger with the increase of annealing temperature, and the quantum confinement effect will become weaker. As a result, the QD band-gap will get smaller, and the first exciton absorption peak will shift to a longer wavelength. Therefore, the wavelength of the first exciton absorption for sample *G*2, expectedly, is longer than that for sample *G*1. Also, we can see that the absorbance increases with the wavelength shorter than the first absorption peak, and this is because more energetic photons can excite electrons from populated regions of the valence band to numerous available states deep in the conduction band. For sample *G*3, no clear absorption peak occurs. As discussed above, one nominal PbSe QD in sample *G*3 is composed of several smaller QDs with different sizes, and the whole sample is actually deemed as containing PbSe QDs with very wide size distribution, which accordingly leads to the missing absorption peak in this sample. In addition, all five samples possess the sudden-drop "terrace" feature around the wavelength of 2,750 nm, and the feature position or amplitude has no obvious variation for the different samples. Thus, we assume that this feature may come from the base glass. In ref [36], Dantas et al. reported a similar feature near the energy of 1.5 eV in their studies on PbS QD-doped silicate glasses, but they ascribed this feature to surface states. In the short wavelength regime around 1,050 nm (850 nm for sample *G*3), the absorbance for the incident light transmitting the glass samples *G*1–*G*3 exceeds 3. In view of the absorbance equation expressed by:

$$A = \log_{10} \frac{I_0}{I} \tag{1}$$

where *A* is the absorbance, *I* is the intensity of the light that have passed through the glass sample and I_0 is the intensity of the incident light. The intensity of the transmitted light only accounts for 1/1,000 of the incident light, indicating that the PbSe QDs-doped glass samples are almost not transparent in the short wavelength around 1,050 nm (850 nm for sample *G*3). However, contrary to the annealed PbSe QDs-doped glasses, both the as-prepared glass samples with and without PbSe introductions are transparent and almost kept constant in absorbance in the measured incident light energy range except for the "terrace" feature. Therefore, it is believed that the light absorption originates from the generated PbSe QDs in glasses mostly, and the absorption from the base glass can be ignored instead.

In order to clearly identify the different optical transitions and the corresponding transition energies, the second derivatives of the absorption spectra of samples *G*1 and *G*2 are made, as shown in the insets of Fig. 2. The minimum in

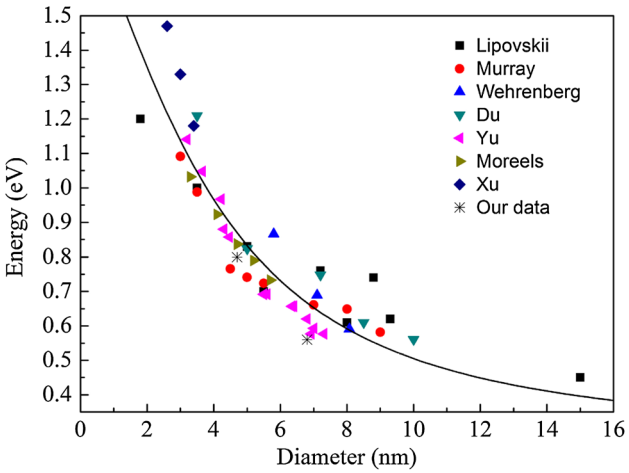

Fig. 3 Band-gap energy of PbSe QDs versus QDs diameter

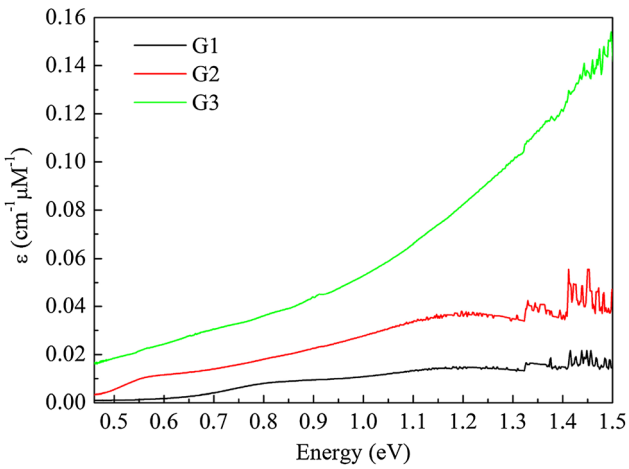

Fig. 4 Molar extinction coefficients of PbSe QDs as a function of incident photon energy

the second derivative corresponds to the absorption peak in the optical absorption spectrum (note that the second derivative is plotted with minimum upwards) [17]. Three minima, namely $1S_h$–$1S_e$, $1S_h$–$1P_e$ (or $1P_h$–$1S_e$) and $1P_h$–$1P_e$ transitions, can be distinguished for samples *G*1 and *G*2, respectively. According to the positions of the minima, the transition energies can be determined exactly. The $1S_h$–$1S_e$ transition energy is generally known as the band-gaps of PbSe QDs, together with the size data of PbSe QDs determined by TEM results mentioned above, so we can get the relation of the band-gap energies of PbSe QDs versus QDs diameters, as shown in the scatter plot marked with asterisks in Fig. 3. As a comparison, the data from other groups are supplied in this scatter plot [5, 13, 16, 37–40]. A fitted regression line is derived based on the scatter plot, with an expression of:

$$E_0 = 0.278 + \frac{1}{0.02888d^2 + 0.0872d + 0.64255} \quad (2)$$

where d (nm) is the mean diameter and E_0 (eV) is the band-gap energy of PbSe QDs. This expression can be used to determine the mean size of PbSe QDs if given the absorption spectrum. Therefore, with the above Eq. (2), the mean QD sizes in samples $G1$ and $G2$ can be determined as 5.2 and 8.6 nm, respectively. For sample $G3$, no clear absorption peak from 1 to 1 s transition can be distinguished in its corresponding absorption spectrum due to the fact that this sample is actually composed of at least three kinds of PbSe QDs with different size distributions, as stated above. Therefore, the QD size in sample $G3$ cannot be determined by the Eq. (2). For discussions below, the QD sizes derived from Eq. (2) were adopted.

In view of the PbSe QDs concentrations in the samples and the thicknesses of the samples, the absorbance curves displayed in Fig. 2 can be transformed into the molar extinction coefficient curves shown in Fig. 4, using the relation:

$$A = \varepsilon c x \quad (3)$$

where A is the absorbance as defined above, ε is the molar extinction coefficient, c is the molar concentration of PbSe QDs and x is the sample thickness. Not surprisingly, the molar extinction coefficients are in an order of $G1 < G2 < G3$ because the grain sizes in sample increase in the order of $G1$, $G2$ and $G3$. In order to avoid the need to calibrate the absorbance for samples with markedly different size dispersions, an energy-integrated molar extinction coefficient for the first exciton transition, $\varepsilon_{\mathrm{gap,eV}}$, is calculated with the method Moreels et al. [13] addressed, which are 1.37 $\mathrm{cm^{-1}}$ meV $\mu\mathrm{M^{-1}}$ for sample $G1$ and 0.59 $\mathrm{cm^{-1}}$ meV $\mu\mathrm{M^{-1}}$ for sample $G2$. From $\varepsilon_{\mathrm{gap,eV}}$, the energy-integrated absorption coefficient is derived according to the equation [13, 20]:

$$\mu_{\mathrm{gap}} = \frac{6}{\pi d^3} \frac{\ln(10)\varepsilon_{\mathrm{gap,eV}}}{N_{\mathrm{A}}} \quad (4)$$

where N_{A} is the Avogadro's constant. Then, the μ_{gap} is calculated to be ~7.1 × 10^4 $\mathrm{cm^{-1}}$ meV for sample $G1$ and ~6.8 × 10^3 $\mathrm{cm^{-1}}$ meV for sample $G2$. These values are only about 1/10 of those from colloidal PbSe QDs previously reported [13], which suggests that the PbSe QDs in glass matrices possess weaker light absorption capacity at near-band-edge wavelengths than QDs in solutions presumably due to the much more surface defect states in former than in later case. In quantum mechanics, a nomenclature, oscillator strength, is usually used as a measure of the relative strength of the electronic transitions within atomic or molecular systems. Based on the μ_{gap}, the oscillator strength per particle f_{if} of the first optical transition can be calculated with the expression of [13]:

$$f_{\mathrm{if}} = \frac{4\varepsilon_0 m_3 c m_{\mathrm{e}}}{\mathrm{e}h} \frac{1}{|f_{\mathrm{LF}}|^2} \frac{\pi d^3}{6} \mu_{\mathrm{gap}} \quad (5)$$

here, ε_0 is the electric constant, m_{e} is the electron mass, e is the electron charge and f_{LF} denotes the local field factor with the expression of:

$$|f_{\mathrm{LF}}|^2 = \frac{9m_3^4}{\left(n_1^2 - k_1^2 + 2m_3^2\right)^2 + 4(n_1 k_1)^2} \quad (6)$$

where m_3 is the refractive index for glass matrix, which is calculated to be 1.522; n_1 and k_1 are refractive index and extinction coefficient, respectively, for bulk PbSe, which are incident light wavelength dependent. For sample $G1$, taking $n_1 - k_1 i = 4.64 - 0.95i$, we can get $f_{\mathrm{if}} = 1.08$; whereas for sample $G2$, we take $n_1 - k_1 i = 4.59 - 0.74i$ [41], and then, we can get $f_{\mathrm{if}} = 0.44$. The calculation results are smaller than 8–25 in previous reports possibly due to the existence of substantial surface defects [13]. Also, note that the oscillator strength from sample $G1$ is larger than that from sample $G2$. This is because the mean size of PbSe QDs in sample $G1$ is smaller than that in sample $G2$, and the overlap between electron and hole wave functions would increase with a decrease in particle size, thus leading to the increase of the oscillator strength [18].

For optical transitions far from any strong resonances and far from the band edge where the QD density of states may be approximated as a continuum; that is, at high photon energy, the absorption behavior of QDs becomes featureless and are essentially unaffected by quantum confinement. According to the previous reports on InAs, CdSe and PbSe QDs, the molar extinction coefficient at high photon energy is proportional to the QD content in matrix, while irrelevant to the QD size [13, 21, 22].Therefore, the absorption spectrum of PbSe QD at high photon energy may be used as a measure of the content of PbSe QD in glass matrix. In Fig. 4, the molar extinction coefficient from sample $G3$ is a good choice for measuring the content of PbSe QDs because it has no apparent first excitonic transition energy, and the absorption behavior of PbSe QD at high photon energy is hardly affected by quantum confinement. The molar extinction coefficient ε is converted to a per particle absorption cross section C_{th} using:

$$C_{\mathrm{th}} = \frac{2303\varepsilon_\lambda}{N_{\mathrm{A}}} \quad (7)$$

we can then get $C_{\mathrm{th}} = 5.853 \times 10^{-13}$ $\mathrm{cm^2}$ at the photon energy of 1.5 eV. The absorption coefficient is obtained according to the expression:

$$\mu_{\mathrm{th}} = \frac{C_{\mathrm{th}}}{\frac{1}{6}\pi d^3} \quad (8)$$

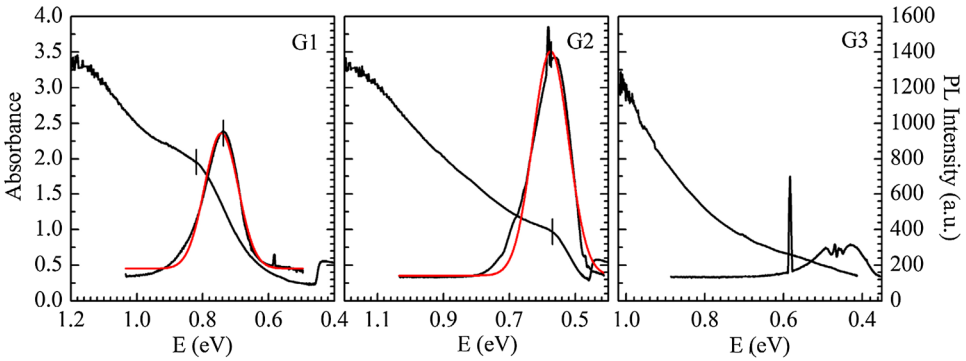

Fig. 5 PL and absorption spectra of samples *G*1, *G*2 and *G*3

accordingly, the result is $\mu_{th} = 8.086 \times 10^4$ cm^{-1}. However, according to the theoretical equation Ricard et al. derived with an expression of [14]:

$$\mu_{th} = \frac{n_1}{m_3} |f_{LF}|^2 \frac{4\pi k_1}{\lambda} \tag{9}$$

where λ is the wavelength of the incident photon. Taking $n_1 - k_1 i = 4.64 - 2.64i$ [41], the theoretical calculation result is $\mu_{th} = 6.098 \times 10^4$ cm^{-1} at the photon energy of 1.5 eV, in roughly agreement with the experimental result, which indicates again that high energy photon transitions between states are essentially unaffected by quantum confinement, and the QD absorption is equivalent to that of bulk materials regardless of the organic solvent or inorganic glass medium surrounding QDs [21, 22].

Figure 5 displays the absorption and PL spectrum of samples *G*1, *G*2 and *G*3, respectively, and the red traces are fitted curves with a Gaussian profile, which corresponds to the respective PL spectra of samples *G*1 and *G*2. As for the PL spectra, it can be seen that clear emissive peaks arise in samples *G*1 and *G*2; while in sample *G*3, the PL peak looks weak and diffused, and it seems that this emissive peak is made up of several peaks, which is consistent with the above TEM and absorption spectra results. Comparing the fitted Gaussian curves and the measured PL spectra, we can see more clearly that the right sides of the PL peaks from samples *G*1 and *G*2 look relatively steep, while the left sides are gentle, that is, the PL is quenched at short wavelengths and enhanced at long wavelengths. This can be ascribed to the Forster energy transfer mechanism. Suppose that the smaller PbSe QDs in sample act as PL "donor" and the larger QDs as PL "acceptor," the emission from the smaller QDs can be reabsorbed by the larger QDs. Therefore, the seeming PL intensity from smaller QDs, reflected in the left side of the PL peak, can be restrained. Clark et al. [19] gave an estimated Forster radius of ~80 Å for the PbS QDs and mentioned that a 50 % uncertainty in the estimation produces only a ~7 Å error in the Forster radius. In view of the similarity between the PbSe and PbS QDs, assuming that the Forster radius of PbSe QDs is ~80 Å cannot cause many errors. According to the above Fig. 1, the average distance between neighboring PbSe QDs is definitely within ~80 Å. Therefore, it is credible that the Forster energy transfer is responsible for the shape of the PL peak. It is mentioned that the sharp peak around 0.59 eV, superimposed in the PL peak, originates from the second order of diffraction because of an excitation laser wavelength of 1,064 nm.

Comparing the absorption spectrum with its corresponding PL spectrum, we found that the Stokes shifts between PL and absorption peaks are about 70 and −7 meV for sample *G*1 and *G*2, respectively. Generally, in case of semiconductor QDs, the magnitude of Stokes shift decreases with the increase of QD size and disappears beyond a certain radius [42–45]. Therefore, reasonably, the PL band is red-shifted with respect to the absorption-edge by a pronounced value of 70 meV for PbSe QDs in a small radius of 5.2 nm. PbSe has a unique electronic structure, whereby both the valance band maximum (VBM) and the conduction band minimum (CBM) are L-like states. The shift is a result of a split of the exciton manifold by the L-valley mixing and by the electron–hole exchange interaction, which further splits into dark and bright states. The splitting increases with decreasing size. In addition, in very small PbSe quantum dots, ionic relaxation upon photoexcitation can lead to large Franck–Condon shifts, which may also contribute to the experimentally observed Stokes shift [44, 46, 47]. Stokes shift is usually known as $2S\hbar\omega_{LO}$ [48], where S is the Huang–Rhys factor, that is roughly being a measure of the strength of the exciton–phonon coupling, $\hbar\omega_{LO}$ is the energy of longitudinal optical (LO) phonon, which is 16.7 meV for PbSe [49]. Then, the S factor is calculated to be 2.1, which suggests that a mean number of 2.1 phonons emit during the relaxation processes after excitation following the absorption of a photon and a vertical optical transition [50]. However, an anti-Stokes photoluminescence (ASPL) with a blue-shift of 7 meV emerges for sample *G*2 with the PbSe QD size increasing up to 8.6 nm. The mechanism for ASPL can be attributed to two-photon absorption, thermal activation by Auger transition or

absorption of phonons [51, 52]. The large magnitude variation of Stokes shift was also reported previously by Lifshitz et al. [24].

4 Conclusions

Contrary to studies on colloidal QDs, few studies were related to QDs in glasses. In this paper, we reported syntheses of PbSe QDs in silicate glasses by a simple melt-annealing technique, and the glass samples were characterized with different characterization techniques such as TEM, absorption and PL spectra methods. TEM results demonstrate the formation of PbSe QDs in glasses; furthermore, it shows that the increased heat-treatment temperature not only promotes the growth of PbSe QDs, but also promotes the generated smaller PbSe QDs to coalesce into bigger ones, which leads to the decrease of QD density in host glass. Then, the absorption and PL studies on PbSe QDs in glasses were investigated qualitatively and quantitatively. The light absorption spectra show that the light absorption originates from the PbSe QDs in glasses mostly. The energy-integrated absorption coefficient for the first exciton transition, μ_{gap}, is calculated to be ~7.1×10^4 cm^{-1} meV for sample $G1$ and ~6.8×10^3 cm^{-1} meV for sample $G2$, which are only about 1/10 of those from colloidal PbSe QDs previously reported, presumably due to the much more surface defect states in embedded PbSe QDs than in colloidal PbSe QDs. The oscillator strength per particle f_{if} of the first optical transition was calculated to be 1.08 for sample $G1$ and 0.44 for sample $G2$, smaller than 8–25 in previous reports possibly due to the existence of substantial surface defects. The PL studies show that the Forster energy transfer is responsible for the shape of the PL peak. Also, the Stokes shift of the PL peak with respect to the absorption-edge was studied; for sample $G1$, a pronounced shift of 70 meV was observed; while for sample $G2$, an ASPL of -7 meV was observed. In summary, the silicate glasses containing PbSe QDs have great practical applications in infrared optoelectronic devices.

Acknowledgments The authors are grateful for the financial support from the Natural Science Foundation of Zhejiang Province (No. LY13F040002), the project of Science and Technology Department of Zhejiang Province (No. 2012R10020-08) and the National Natural Science Foundation of China (No. 61274124, No. 61474100); DWM also thanks for the financial support from the China Scholarship Council.

References

1. D.V. Talapin, J.S. Lee, M.V. Kovalenko, E.V. Shevchenko, Chem. Rev. **110**, 389 (2010)
2. J.A. Smyder, T.D. Krauss, Mater. Today **14**, 382 (2011)
3. F.W. Wise, Acc. Chem. Res. **33**, 773 (2000)
4. E. Lifshitz, M. Bashouti, V. Kloper, A. Kigel, M. Eisen, S. Berger, Nano Lett. **3**, 857 (2003)
5. A. Lipovskii, E. Kolobkova, V. Petrikov, I. Kang, A. Olkhovets, T. Krauss, M. Thomas, J. Silcox, F. Wise, Q. Shen, S. Kycia, Appl. Phys. Lett. **71**, 3406 (1997)
6. G. Dong, B. Wu, F. Zhang, L. Zhang, M. Peng, D. Chen, E. Wu, J. Qiu, J. Alloys Compd. **509**, 9335 (2011)
7. M. Pinczolits, G. Springholz, G. Bauer, Appl. Phys. Lett. **73**, 250 (1998)
8. D.A. Carder, A. Markwitz, R.J. Reeves, J. Kennedy, F. Fang, Nucl. Instrum. Methods Phys. Res. B **307**, 154 (2013)
9. R. Erce-Montilla, M. PiÑero, N. de la Rosa-Fox, A. Santos, L. Esquivias, J. Mater. Res. **16**, 2572 (2001)
10. M. Brumer, A. Kigel, L. Amirav, A. Sashchiuk, E. Lifshitz, Adv. Funct. Mater. **15**, 1111 (2005)
11. O.E. Semonin, J.C. Johnson, J.M. Luther, A.G. Midgett, A.J. Nozik, M.C. Beard, J. Phys. Chem. Lett. **1**, 2445 (2010)
12. C. Cheng, H. Jiang, D. Ma, X. Cheng, Opt. Commun. **284**, 4491 (2011)
13. I. Moreels, K. Lambert, D.D. Muynck, F. Vanhaecke, D. Poelman, J.C. Martins, G. Allan, Z. Hens, Chem. Mater. **19**, 6101 (2007)
14. I. Moreels, Z. Hen, Small **4**, 1866 (2008)
15. Q. Dai, Y. Wang, X. Li, Y. Zhang, D.J. Pellegrino, M. Zhao, B. Zou, J. Seo, Y. Wang, W.W. Yu, ACS Nano **3**, 1518 (2009)
16. B.L. Wehrenberg, C. Wang, P. Guyot-Sionnest, J. Phys. Chem. B **106**, 10634 (2002)
17. R. Koole, G. Allan, C. Delerue, A. Meijerink, D. Vanmaekelbergh, A.J. Houtepen, Small **4**, 127 (2008)
18. L. Cademartiri, E. Montanari, G. Calestani, A. Migliori, A. Guagliardi, G.A. Ozin, J. Am. Chem. Soc. **128**, 10337 (2006)
19. S.W. Clark, J.M. Harbold, F.W. Wise, J. Phys. Chem. C **111**, 7302 (2007)
20. I. Moreels, K. Lambert, D. Smeets, D.D. Muynck, T. Nollet, J.C. Martins, F. Vanhaecke, A. Vantomme, C. Delerue, G. Allan, Z. Hens, ACS Nano **3**, 3023 (2009)
21. P. Yu, M.C. Beard, R.J. Ellingson, S. Ferrere, C. Curtis, J. Drexler, F. Luiszer, A.J. Nozik, J. Phys. Chem. B **109**, 7084 (2005)
22. C.A. Leatherdale, W.K. Woo, F.V. Mikulec, M.G. Bawendi, J. Phys. Chem. B **106**, 7619 (2002)
23. J.M. Pietryga, R.D. Schaller, D. Werder, M.H. Stewart, V.I. Klimov, J.A. Hollingsworth, J. Am. Chem. Soc. **126**, 11752 (2004)
24. E. Lifshitz, M. Brumer, A. Kigel, A. Sashchiuk, M. Bashouti, M. Sirota, E. Galun, Z. Burshtein, A.Q. Le Quang, I. Ledoux-Rak, J. Zyss, J. Phys. Chem. B **110**, 25356 (2006)
25. P.T. Guerreiro, S. Ten, N.F. Borrelli, J. Butty, G.E. Jabbour, N. Peyghambarian, Appl. Phys. Lett. **71**, 1595 (1997)
26. J.F. Philipps, T. Töpfer, H. Ebendorff-Heidepriem, D. Ehrt, R. Sauerbrey, N.F. Borrelli, Appl. Phys. B **72**, 175 (2001)
27. V.G. Savitski, A.M. Malyarevich, K.V. Yumashev, B.D. Sinclair, A.A. Lipovskii, Appl. Phys. B **76**, 253 (2003)
28. L.A. Padilha, A.A.R. Neves, C.L. Cesar, L.C. Barbosa, C.H. Brito, Cruz. Appl. Phys. Lett. **85**, 3256 (2004)
29. R.S. Silva, P.C. Morais, A.M. Alcalde, F. Qu, A.F.G. Monte, N.O. Dantas, J. Non-Cryst. Solids **352**, 3522 (2006)
30. A.M. Malyarevich, M.S. Gaponenko, V.G. Savitski, K.V. Yumashev, G.E. Rachkovskaya, G.B. Zakharevich, J. Non-Cryst. Solids **353**, 1195 (2007)
31. Chao Liu, Y.K. Kwon, J. Heo, J. Non-Cryst. Solids **355**, 1880 (2009)
32. A. Dementjev, V. Gulbinas, Opt. Mater. **31**, 647 (2009)
33. P.A. Loiko, G.E. Rachkovskaya, G.B. Zacharevich, K.V. Yumashev, J. Lumin. **143**, 418 (2013)
34. D.W. Ma, C. Cheng, J. Am. Ceram. Soc. **96**, 1428 (2013)
35. N.O. Dantas, F. Qu, A.F.G. Monte, R.S. Silva, P.C. Morais, J. Non-Cryst. Solids **352**, 3525 (2006)

36. N.O. Dantas, F. Qu, R.S. Silva, P.C. Morais, J. Phys. Chem. B **106**, 7453 (2002)
37. C.B. Murray, S.H. Sun, W. Gaschler, H. Doyle, T.A. Betley, C.R. Kagan, IBM J. Res. Dev. **45**, 47 (2001)
38. H. Du, C.L. Chen, R. Krishnan, T.D. Krauss, J.M. Harbold, F.W. Wise, M.G. Thomas, J. Silcox, Nano Lett. **2**, 1321 (2002)
39. W.W. Yu, J.C. Falkner, B.S. Shih, V.L. Colvin, Chem. Mater. **16**, 3318 (2004)
40. K. Xu, J. Heo, Phys. Scr. **T139**, 014062 (2010)
41. E.D. Palik, *Handbook of optical constants of solids* (Academic Press, New York, 1985)
42. A. Bagga, P.K. Chattopadhyay, S. Ghosh The 14th International Workshop on the Physics of Semiconductor Devices, 1 (2007)
43. A.L. Rogach, T. Franzl, T.A. Klar, J. Feldmann, N. Gaponik, V. Lesnyak et al., J. Phys. Chem. C **111**, 14628 (2007)
44. A. Kigel, M. Brumer, G. Maikov, A. Sashchiuk, E. Lifshitz, Superlattices Microstruct. **46**, 272 (2009)
45. I.M. Kupchak, D.V. Korbutyak, S.M. Kalytchuk, YuV Kryuchenko, A. Chkrebtii, J. Phys. Stud. **14**, 2701 (2010)
46. J.M. An, A. Franceschetti, S.V. Dudiy, A. Zunger, Nano Lett. **6**, 2728 (2006)
47. M. Califano, A. Franceschetti, A. Zunger, Nano Lett. **5**, 2360 (2005)
48. P. Nandakumar, C. Vijayan, Y.V.G.S. Murti, J. Appl. Phys. **91**, 1509 (2002)
49. R.D. Schaller, J.M. Pietryga, S.V. Goupalov, M.A. Petruska, Phys. Rev. Lett. **95**, 196401 (2005)
50. A.D. Yoffe, Adv. Phys. **50**, 1 (2001)
51. Yu.P. Rakovich, S.A. Filonovich, M.J.M. Gomes, J.F. Donegan, D.V. Talapin, A.L. Rogach et al., Phys. Stat. Sol. B **229**, 449 (2002)
52. S.K. Tripathy, G. Xu, X. Mu, Y.J. Ding, M. Jamil, R.A. Arif et al., Appl. Phys. Lett. **93**, 201107 (2008)